I&EC research
Industrial & Engineering Chemistry Research

Article

pubs.acs.org/IECR

The Solvation and Dissociation of 4-Benzylaniline Hydrochloride in Chlorobenzene

Emma K. Gibson,[†] John M. Winfield,[†] David Adam,[†] Alice A. Miller,[‡] Robert H. Carr,[§] Archie Eaglesham,[§] and David Lennon*[,†]

[†]School of Chemistry, Joseph Black Building, University of Glasgow, Glasgow, United Kingdom G12 8QQ.

[‡]School of Computing Science, Sir Alwyn Williams Building, University of Glasgow, Glasgow, United Kingdom G12 8QQ.

[§]Huntsman (Europe) BVBA, Everslaan 45, 3078 Everberg, Belgium

Supporting Information

ABSTRACT: A reaction scheme is proposed to account for the liberation of 4-benzylaniline from 4-benzylaniline hydrochloride, using chlorobenzene as a solvent at a temperature of 373 K. Two operational regimes are explored: "closed" reaction conditions correspond to the retention of evolved hydrogen chloride gas within the reaction medium, whereas an "open" system permits gaseous hydrogen chloride to be released from the reaction medium. The solution phase chemistry is analyzed by ^{1}H NMR spectroscopy. Complete liberation of solvated 4-benzylaniline from solid 4-benzylaniline hydrochloride is possible under "open" conditions, with the entropically favored conversion of solvated hydrogen chloride to the gaseous phase thought to be the thermodynamic driver that effectively controls a series of interconnecting equilibria. A kinetic model is proposed to account for the observations of the open system.

1. INTRODUCTION

Polyurethanes have wide application in society, being used in such diverse areas as the automotive, construction, furnishing, and surface coating industries.[1−3] Increasingly, they are finding wide application as insulation agents. They may be prepared from isocyanates, which are typically obtained by the phosgenation of aromatic amines in the presence of chlorobenzene as a solvent.[1,2,4,5] Methylene diphenyl diisocyanate (MDI) is the major isocyanate used, with a total global production capacity of ∼5 Mt in 2011.[6,7]

Isocyanate production initially involves phosgenation of an amine to form a carbamoyl chloride, which subsequently decomposes to form the desired isocyanate (eqs 1 and 2).[2,4,5]

$$RNH_2 + COCl_2 \rightarrow RNHC(O)Cl + HCl \quad (1)$$

$$RNHC(O)Cl \rightarrow RNCO + HCl \quad (2)$$

However, hydrogen chloride is released at each stage and undergoes a side reaction with aromatic amine starting material to form an unwanted hydrochloride salt (eq 3).[1,4,5]

$$RNH_2 + HCl \rightarrow RNH_3Cl \quad (3)$$

The amine hydrochloride precipitate is insoluble in the reaction medium and, unless treated, could lead to a significant yield loss within the process. However, the precipitate reacts slowly and endothermically with phosgene to produce the desired isocyanate (eq 4).[1,2,4]

$$RNH_3Cl + COCl_2 \rightarrow RNCO + 3HCl \quad (4)$$

The processing of the amine hydrochloride precipitate constitutes a resource intensive process,[1,2,4,5] so an improved understanding of the decomposition of the hydrochloride salt (the back reaction of eq 3) is appropriate and could lead to improvements in the efficiency of the isocyanate production process; this issue is examined in the present work.

Previous work by Gibson et al. has reported on the structural and spectroscopic characteristics associated with the hydrochlorination of 4-benzylaniline[8] and 4,4′-methylenedianiline[6] in chlorobenzene. Badawi has recently analyzed the structure and vibrational spectra of 4,4′-methylenedianiline.[9] The work of Gibson et al. showed the dissolution of hydrogen chloride gas in chlorobenzene required rigorous mixing and, even then, it was only sparingly soluble.[8] This communication is concerned with liberating 4-benzylaniline (4-BA, $C_6H_5CH_2C_6H_4NH_2$), a model compound with chemical functionality representative of reagents used in certain isocyanate production chains,[8] from 4-benzylaniline hydrochloride (4-BA.HCl, $C_6H_5CH_2C_6H_4NH_3^+Cl^-$) (eq 5).

$$\text{4-BA.HCl}_{(s)} \xrightarrow{\text{chlorobenzene}} \text{4-BA}_{(solv)} + \text{HCl}_{(solv)} \quad (5)$$

where the subscripts "(s)" and "(solv)" signify solid and solvated species respectively. Reflecting the industrial operation,[1,4] chlorobenzene is used as the solvent.

Despite the relevance of eq 5 to the operation of large-scale production facilities, there is a paucity of literature on the factors influencing liberation of the aromatic amine in a representative process solvent. Liberation of starting material (4-BA) from byproduct (4-BA.HCl) might be achievable by varying the reactor configuration during dissolution experiments. Scheme 1 presents a three-stage reaction scheme as one possibility. First, solid 4-BA.HCl is solvated (4-BA.HCl$_{(solv)}$),

Received: November 5, 2013
Revised: February 20, 2014
Accepted: February 22, 2014
Published: February 23, 2014

   dx.doi.org/10.1021/ie403745s | Ind. Eng. Chem. Res. 2014, 53, 4156−4164

Scheme 1. A Possible Reaction Scheme for the Dissolution of Solid 4-BA.HCl in Chlorobenzene[a]

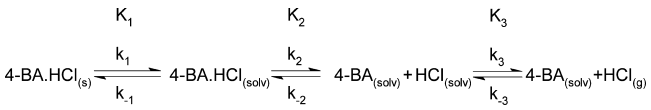

[a] K_1 is the equilibrium constant corresponding to the solvation of 4-BA.HCl from solid 4-BA.HCl, with k_1 and k_{-1} being the associated respective forward and backward rate coefficients. K_2 is the equilibrium constant corresponding to the dissociation of solvated 4-BA.HCl, with k_2 and k_{-2} being the associated respective forward and backward rate coefficients. K_3 is the equilibrium constant corresponding to the partitioning of solvated HCl into the vapor phase, with k_3 and k_{-3} being the associated respective forward and backward rate coefficients.

then 4-BA.HCl$_{(solv)}$ dissociates to form solvated 4-BA and hydrogen chloride (4-BA$_{(solv)}$ and HCl$_{(solv)}$), and then finally, the solvated hydrogen chloride partitions into the gaseous phase (HCl$_{(g)}$). This article examines the feasibility of Scheme 1 and considers the effect of laboratory reactor configurations that facilitate either (i) the retention of HCl within the reaction environment (this constitutes a "closed" system) or (ii) the release of gaseous HCl from the reaction environment (this constitutes an "open" system). A kinetic model is proposed to account for the trends observed experimentally with the open reaction system. These actions lead to an improved understanding of a pathway within the complexity of industrial-scale phosgenation process chemistry.

Our interest in the behavior of HCl coincides with a resurgence of academic and industrial activity surrounding the Deacon reaction, where HCl is oxidized to Cl_2 (eq 6).[10]

$$4HCl + O_2 \rightarrow 2H_2O + 2Cl_2 \quad (6)$$

Following work announced by Sumitomo,[11] recent studies have examined a range of new materials that display favorable properties as efficient Deacon catalysts.[12−17] In principle, these improvements in the operation of the Deacon reaction could be applied to convert waste HCl produced in the industrial synthesis of aryl isocyanates to Cl_2, which could then be used as a feedstock for phosgene production. Phosgene synthesis typically involves the reaction of CO and Cl_2 over a high-surface-area carbon catalyst.[18,19] That body of work is supplemented by studies investigating the feasibility of phosgene production via the oxy-chlorination of CO.[20−22] Although the aforementioned studies on a new generation of Deacon catalysts and CO oxy-chlorination routes to phosgene are more closely linked to initiatives to help close the chlorine cycle,[23] the work reported here primarily seeks to evaluate the feasibility of a new route to workup hydrochloride salt byproducts associated with large-scale isocyanate unit operations.

2. EXPERIMENTAL SECTION

Samples of solid 4-benzylaniline hydrochloride, 4-BA.HCl$_{(s)}$, were prepared and characterized by ^{1}H NMR and FTIR spectroscopy, as described previously.[8] The melting point was mp = 453 K, which is consistent with a previous report[8] and thermogravimetric analysis showed negligible mass loss below 403 K. Thus, in order to maximize 4-BA.HCl solubility while avoiding the possibility of thermal decomposition of the starting material, dissolution measurements in chlorobenzene (boiling point of bp = 415 K) were performed at 373 K. Numerical fitting routines were configured within the Origin graphical software package (OriginLab Corporation, Version 7.5). The reference compound 4-benzylaniline (Alfa-Aesar, purity 98%) was used as received; mp = 313 K.

2.1. Dissolution Studies. Reactions were performed within a fume cupboard using a Radley's Carousel 6 reaction station (Radley's Discovery Technologies) with 25 cm^3 flasks and a head space above solution of 75 cm^3. The carousel housed six reaction vessels, each treated to identical mixing (baffled flasks and cross-shaped stirrer bars) and temperature conditions. Each reactor was connected to a condenser unit. Continuous mixing was maintained at all times at a rate so as to sustain a vortex in the liquid phase that facilitated vigorous exchange between the gas/liquid and solid/liquid interfaces. A more-detailed description of the apparatus is presented in section S-1 of the Supporting Information (Figures S1 and S2).

Two reactor configurations were adopted. First, for operation in a "closed" configuration, the reactor was sealed and liquid samples were extracted for analysis by means of a syringe sampling through a polytetrafluoroethylene (PTFE) septum. This arrangement prevented gaseous hydrogen chloride from leaving the reaction environment, i.e., liquid plus headspace. Second, for an "open" configuration, the septum was simply removed from the top of the reactor and the valve opened, so that any gaseous hydrogen chloride would be irreversibly expelled from the reaction medium.

Chlorobenzene (15 cm^3, Aldrich, purity 99.8%, <0.005% water) with 4-BA.HCl in each of the six carousel flasks was maintained at 373 K for periods up to 25 h. For the closed series of experiments, ∼0.03 g of 4-BA.HCl was used (9.10 mmol dm^{-3}); for the open experiments, ∼0.02 g of 4-BA.HCl was used (6.07 mmol dm^{-3}). Liquid samples taken by syringe were filtered using Whatman inorganic Anotop syringe filters (0.2 μm porosity) before NMR analysis. Blank measurements, where a thermocouple was placed in each flask, confirmed that the reaction temperature was maintained at 373 K throughout the duration of the solubilization experiments.

2.2. Quantitative ^{1}H NMR Spectroscopy. ^{1}H NMR spectra were recorded using a Bruker Avance 400 MHz spectrometer. The solubility of 4-BA in chlorobenzene at 298 K is 4.722 (±0.034) mol dm^{-3}, whereas the solubility of 4-BA.HCl in chlorobenzene at 293 K is 0.26 (±0.13) mmol dm^{-3} and rises to 0.52 (±0.19) mmol dm^{-3} at 333 K.[8] A conventional single pulse ^{1}H NMR spectrum collected using 8000 scans over an 8 h period afforded a detection limit of only 0.1 mmol dm^{-3}, which is insufficient to analyze 4-BA.HCl$_{(solv)}$. Thus, in order to improve sensitivity, a solvent suppression pulse program[24,25] was deployed to suppress the otherwise dominant chlorobenzene resonance. Presaturation of chlorobenzene resonances at 6.939 and 7.092 ppm was achieved using a power level of 60 db and a pulse length of 3 s. These arrangements afforded a 10-fold enhancement in detection limit over an acquisition time of 30 min, albeit with some loss of signal stability. Figure S3 in section S-2 of the Supporting Information presents ^{1}H NMR spectra that demonstrate the benefits of applying the aforementioned solvent suppression pulse sequence to investigate low concentrations of aromatic amines in chlorobenzene.

Quantification of spectral intensity was obtained in two ways. First, an NMR glass capillary was used, which contained a measured quantity of dichloromethane in C_6D_6 into the NMR sample tube. The use of deuterated benzene as a solvent for the internal reference avoided any spectral overlap in the 2−6 ppm region of the spectrum, where the diagnostic methylene and

dx.doi.org/10.1021/ie403745s | Ind. Eng. Chem. Res. 2014, 53, 4156−4164

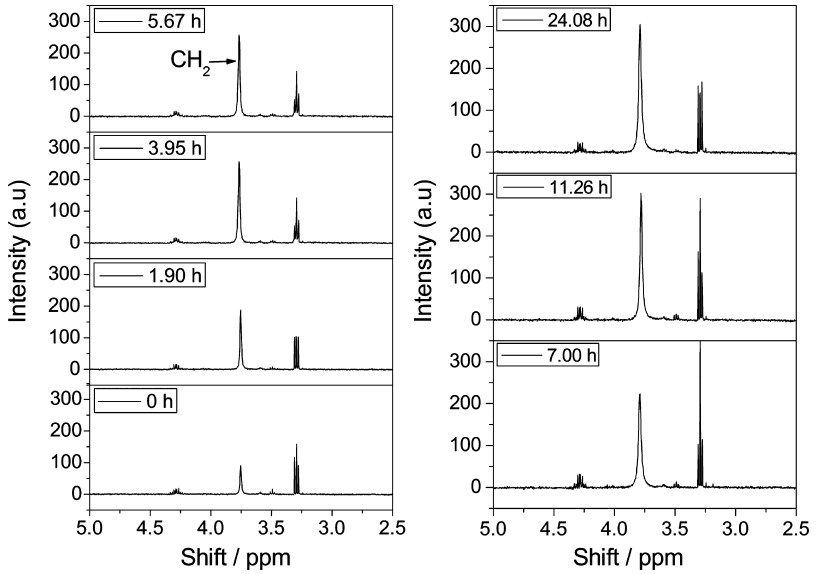

Figure 1. Solution-phase ^{1}H NMR spectra of a mixture of 4-BA.HCl$_{(s)}$ and chlorobenzene as a function of time at 373 K in a stirred and sealed reactor (closed reaction conditions). The CH_2 resonance is observed at 3.76 ppm. The times displayed on each spectrum represent the sampling times after commencement of reaction. Signals at 3.26 and 4.26 ppm are due to impurities in the reaction medium.

amine resonances are located. The use of the glass insert ensured no interaction between the deuterated solvent and the reference material with the reaction mixture. Second, calibration curves were constructed that enabled the integrated spectral response of the methylene and amine protons to be correlated with 4-BA concentration in chlorobenzene. A representative calibration curve is presented in Section S-3 in the Supporting Information (Figure S4). Spectroscopic measurements undertaken using a variety of pulse lengths and delays between successive pulses confirmed relaxation effects were not perturbing spectral intensity.[24,25] Experiments were performed at least in duplicate, with the datasets presented here being representative of all measurements.

Blank experiments were performed using solutions of 4-BA at concentrations comparable to the saturation limit of 4-BA.HCl. Occasionally, one of a set of six measurements would display a minor discontinuity in intensity, attributed to instabilities in the phase matching of the solvent suppression program.[25] Peak intensities were determined by integration of the relevant spectral features. Resonances of the $-CH_2-$ and $-NH_2$ groups appeared at 3.6 and ~3.0 ppm, respectively. The latter resonance was relatively broad, indicating a degree of exchange with protonic material. Infrared spectroscopy has shown the presence of a small number of water molecules to be inherently present in the chlorobenzene solvent;[8] thus, it is assumed that the exchange between these highly dispersed water molecules and the amine groups of 4-BA$_{(solv)}$ is responsible for the broadening of the amine resonance. The issue of exchange processes affecting the shape of the amine NMR resonance is considered more comprehensively in Section S-4 of the Supporting Information (Figure S5). For the open system measurements, all of the solid 4-BA.HCl was solvated for times exceeding ~10 h and the integrated $-CH_2-$ and $-NH_2$ resonances were normalized to a plateau value that corresponded to the original 4-BA.HCl concentration (6.00 ± 0.10 mmol dm^{-3}). This scaling of a single dataset enabled a correction for the variance in the absolute intensities obtained when applying the solvent suppression pulse sequence between different experimental runs.

3. RESULTS

3.1. The Closed System. Figure 1 shows the ^{1}H NMR spectrum of 4-BA.HCl$_{(s)}$ in chlorobenzene at 373 K, as a function of time; this figure shows a sequential growth in intensity of the CH_2 resonance at 3.76 ppm. No signal due to a NH_2 resonance at ~3 ppm[8] is observed in any of the spectra. Calibration measurements using the integrated intensity of the methylene resonance of 4-BA (see the Supporting Information) indicate that the spectral acquisition conditions used here yield a detection limit of 0.01 mmol dm^{-3}. From Scheme 1, the CH_2 resonance could correspond to the combined concentration of 4-BA$_{(solv)}$ and 4-BA.HCl$_{(solv)}$, whereas the NH_2 resonance represents solely 4-BA$_{(solv)}$. Therefore, it is assumed that the CH_2 signal represents 4-BA.HCl$_{(solv)}$ exclusively for the spectra presented in Figure 1. It is acknowledged that impurity peaks are observable in Figure 1, the presence of which could be intermittent. This topic is briefly considered in Section S-5 of the Supporting Information.

Calibration of the NMR spectra presented in Figure 1 leads to the concentration profile displayed in Figure 2. Associating the CH_2 signal solely to 4-BA.HCl$_{(solv)}$, the concentration increases quite rapidly in the first 5 h; thereafter, it rises more slowly, approaching a saturation value ca. 2.25 mmol dm^{-3} after 24 h. The data are well described by an exponential growth function (eq 7):[26]

$$[\text{4-BA.HCl}_{(solv)}]_t = [\text{4-BA.HCl}_{(solv)}]_\infty [1 - \exp(-k_1 t)] \quad (7)$$

where $[\text{4-BA.HCl}_{(solv)}]_t$ and $[\text{4-BA.HCl}_{(solv)}]_\infty$ are, respectively, the concentration of 4-BA.HCl$_{(solv)}$ at time t and at saturation, and k_1 is the rate coefficient for the dissolution process, as described in Scheme 1.

The solid line in Figure 2 represents a least-squares fit of the CH_2 resonance data to eq 7, with the evident goodness of fit suggesting that the 4-BA.HCl dissolution process conforms to first-order kinetics. It might be expected that the dissolution of 4-BA.HCl$_{(s)}$ would follow zero-order kinetics, as is often encountered, for instance, in drug release systems.[27] However,

dx.doi.org/10.1021/ie403745s | Ind. Eng. Chem. Res. 2014, 53, 4156−4164

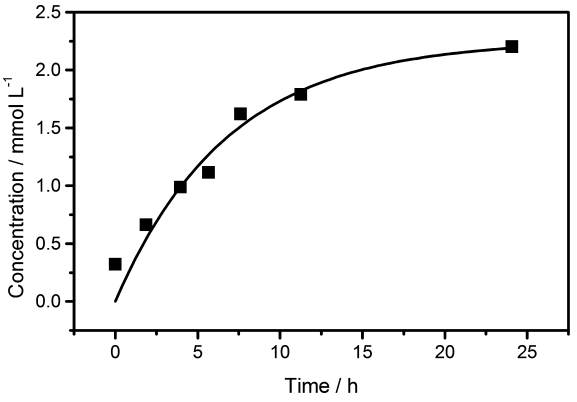

Figure 2. Concentrations associated with the CH_2 ^1H NMR signals for a mixture of 4-BA.HCl(s) and chlorobenzene at 373 K as a function of time in a stirred and sealed reactor. The solid line represents a least-squares fit of the CH_2 resonance to a first-order exponential growth function (eq 7).

one reason for the present outcome could be the limited solubility of the hydrochloride salt in the process solvent.[8]

Equation 6 can be redefined in terms of expressing 4-BA.HCl$_{(solv)}$ as the product (eq 8).

$$\ln\left(1 - \frac{[\text{4-BA.HCl}_{(solv)}]_t}{[\text{4-BA.HCl}_{(solv)}]_\infty}\right) = -k_1 t \tag{8}$$

Figure 3 shows a plot of the first-order integrated rate equation for product formation for four separate runs. With the

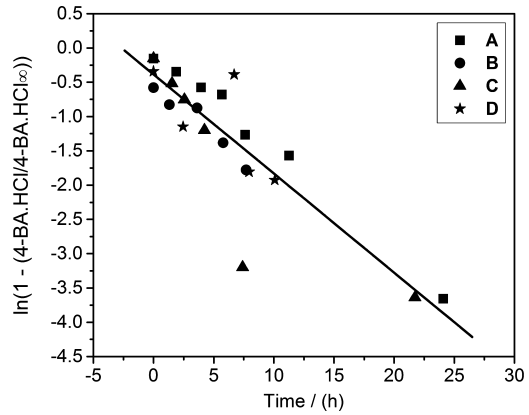

Figure 3. First-order product plot for 4-BA.HCl$_{(solv)}$, as a function of time at 373 K in chlorobenzene under closed conditions. Four experimental data sets are presented, designated A–D. The straight line represents the optimum fit for all of the data points.

exception of a single data point, the dataset is well-correlated to a linear fit, consistent with a first-order process; k_1 = 2.4 (±0.3) × 10^{-3} min^{-1} and [4-BA.HCl$_{(solv)}$]$_\infty$ = 1.87 (±0.53) mmol dm^{-3}. The errors correspond to 1 standard deviation in the determination of the mean rate coefficient and salt saturation value from four separate runs. It is noted that nondissolved 4-BA.HCl$_{(s)}$ was present at the end of all four reactions, as evidenced by the presence of solid particles in the solution. The saturation limit observed here is higher than reported previously at a broadly comparable temperature [0.52 (±0.19) mmol dm^{-3} at 333 K].[8] However, the original measurements were made using a different vessel, indicating some sensitivity of 4-BA.HCl solubility to temperature, reactor configuration and, possibly, residual water.

The data presented above may be used to estimate the equilibrium constant associated with the dissociation of 4-BA.HCl$_{(solv)}$, K_2 (Scheme 1). Equation 9 represents a definition of K_2.

$$K_2 = \frac{[\text{4-BA}_{(solv)}][\text{HCl}_{(solv)}]}{[\text{4-BA.HCl}_{(solv)}]} \tag{9}$$

Assuming [4-BA$_{(solv)}$] ≤ 0.01 mmol dm^{-3}, [HCl$_{(solv)}$] must also be ≤0.01 mmol dm^{-3}. Given that 4-BA.HCl saturates at 1.87 mmol dm^{-3}, then from eq 9, $K_2 < 5.35 \times 10^{-8}$ mol dm^{-3}. It is concluded that closed conditions do not favor the efficient liberation of 4-BA.

3.2. The Open System. In the open configuration, septa at the top of each of the six reactors were removed and the valve opened, so that any gaseous material, specifically HCl$_{(g)}$ (Scheme 1), released into the headspace above the solution phase, was vented to the atmosphere. A mixture of 4-BA.HCl was combined with chlorobenzene (corresponding to a concentration of 6.07 mmol dm^{-3}), maintained at 373 K under conditions of continuous stirring, as described in section 2.1, and analyzed by ^1H NMR spectroscopy as a function of time. The NMR spectra are presented in Figure 4. The concentration values corresponding to the resulting CH_2 and NH_2 resonances are presented in Figure 5.

Figure 5a shows the profile for the CH_2 resonance to be significantly different to that observed in a closed system (Figure 2). Up to ∼7 h, the time for the growth of intensity of the methylene resonance is linear, consistent with zero-order kinetics, and, thereafter it plateaus at ∼6 mmol dm^{-3}. Furthermore, in marked contrast to the closed system, Figures 4 and 5b show the NH_2 resonance to be evident, displaying an almost sigmoid-like dependence on time. For a period of up to ∼6 h, the concentration of 4-BA$_{(solv)}$ increases quite slowly then abruptly rises to maximum intensity at ∼6 mmol dm^{-3}, where it also plateaus.

The NH_2 resonance signifies the presence of 4-BA. When both the CH_2 and NH_2 resonances are observed, as is the case with Figure 5, then the presence of the CH_2 resonance corresponds to a contribution from 4-BA.HCl$_{(solv)}$ and 4-BA$_{(solv)}$. Therefore, in an open system, the concentration associated with the $\delta(CH_2)$ signal at any time t, $[\delta(CH_2)]_t$, and the associated concentration of the $\delta(NH_2)$ signal, $[\delta(NH_2)]_t$, are respectively given by eqs 10 and 11.

$$[\delta(CH_2)]_t = [\text{4-BA.HCl}_{(solv)}]_t + [\text{4-BA(solv)}]_t \tag{10}$$

$$[\delta(NH_2)]_t = [\text{4-BA}_{(solv)}]_t \tag{11}$$

Thus, the concentration of solvated 4-BA.HCl at any time t, $[\text{4-BA.HCl}_{(solv)}]_t$, is given by eqs 12 and 13.

$$[\delta(CH_2)]_t - [\delta(NH_2)]_t = \{[\text{4-BA.HCl}_{(solv)}]_t + [\text{4-BA}_{(solv)}]_t\} - [\text{4-BA}_{(solv)}]_t \tag{12}$$

$$[\delta(CH_2)]_t - [\delta(NH_2)]_t = [\text{4-BA.HCl}_{(solv)}]_t \tag{13}$$

Application of eq 13 leads to the values of 4-BA.HCl$_{(solv)}$ presented in Figure 5b (data points shown as triangles). Here, the 4-BA.HCl$_{(solv)}$ content increases to a maximum of ∼3.5 mmol dm^{-3}, then progressively declines to zero concentration.

dx.doi.org/10.1021/ie403745s | Ind. Eng. Chem. Res. 2014, 53, 4156–4164

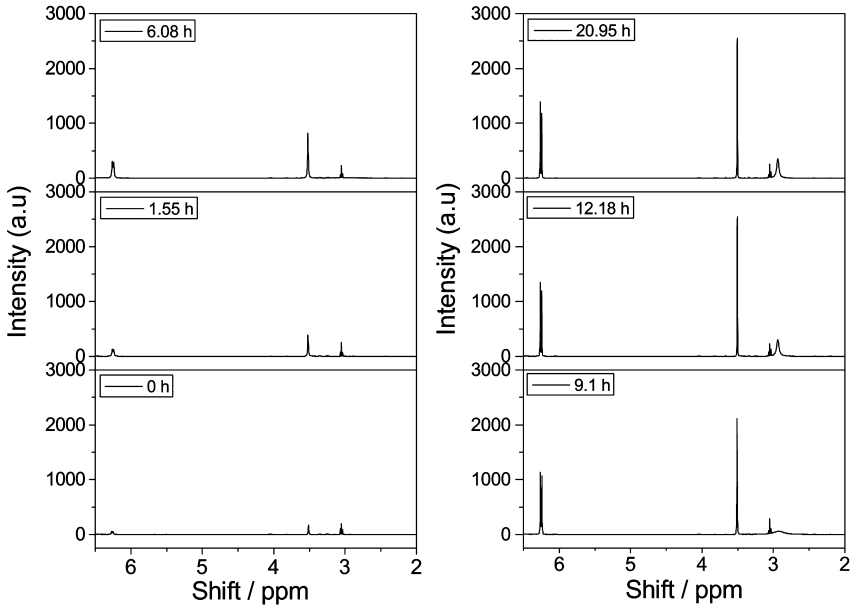

Figure 4. Solution-phase ^{1}H NMR spectra of a mixture of 4-BA.HCl(s) and chlorobenzene as a function of time at 373 K in a stirred and open reactor. The CH_2 and NH_2 resonances are observed at 3.51 and 2.95 ppm, respectively. The times displayed on each spectrum represent the sampling times after commencement of reaction. The signal at 6.20 ppm is unassigned and is attributed to an impurity in the reaction medium.

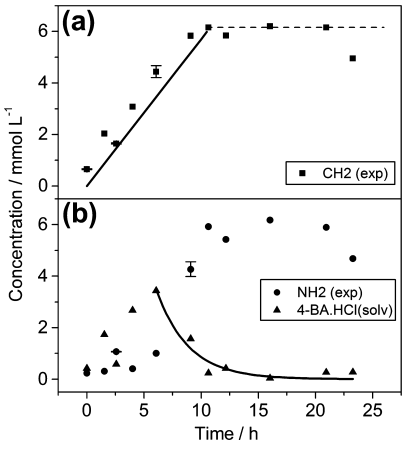

Figure 5. (a) Concentrations associated with the CH_2 ^{1}H NMR signals for a mixture of 4-BA.HCl$_{(s)}$ and chlorobenzene at 373 K, as a function of time in a stirred and open reactor. The solid line represents a linear fit to the CH_2 resonance in the time period of 0−7 h, and the dashed line indicates a plateau concentration value at extended times. (b) Concentrations associated with the NH_2 ^{1}H NMR signals for a mixture of 4-BA.HCl$_{(s)}$ and chlorobenzene at 373 K, as a function of time in a stirred and open reactor. The triangles signify the concentration of 4-BA.HCl$_{(solv)}$ calculated according to eq 13. The solid line represents a fit of the calculated [4-BA.HCl$_{(solv)}$] concentration in the time period of 6−23 h to a first-order exponential decay as signified by eq 14 (presented later in this paper). The error bars represent one standard deviation of the mean from four replicate measurements of standard solutions.

The solid line in Figure 5b is a fit of a single exponential decay, as defined by eq 14, for the data collected in the period of 6−24 h.

$$[\text{4-BA.HCl}_{(solv)}]_t = [\text{4-BA.HCl}_{(solv)}]_{max} \exp(-k_2 t) \quad (14)$$

where $[\text{4-BA.HCl}_{(solv)}]_{max}$ is the maximum concentration of 4-BA.HCl$_{(solv)}$ at mixing time t', and k_2 is the rate coefficient for the dissociation process, as described in Scheme 1. From Figure 5b, $[\text{4-BA.HCl}_{(solv)}]_{max}$ = 3.43 (±0.52) mmol dm^{-3} at t' = 6.08 h. The error in $[\text{4-BA.HCl}_{(solv)}]_{max}$ represents one standard deviation from four replicate concentration measurements of standard solutions of 4-BA. The profile of the calculated 4-BA.HCl$_{(solv)}$ data over the 6−24 h period is well-described by the fit to eq 14, indicating that the dissociation process (eq 15) is consistent with a first-order decay process.

$$\text{4-BA.HCl}_{(solv)} \rightarrow \text{4-BA}_{(solv)} + \text{HCl}_{(solv)} \quad (15)$$

The trends evident in Figure 5 may be rationalized with reference to Scheme 1. The initial dissolution stage (K_1) requires a breakup of the 4-BA.HCl lattice. The dissociation stage (K_2) involves breaking apart the tight ion pair of the solvated hydrochloride salt. The last stage (K_3) is entropically driven, with the transition from solvated to gaseous HCl representing a large increase in entropy. The fact that 4-BA has a high solubility in chlorobenzene[8] means that if redissolution of HCl (k_{-3}) is disfavored, then significant quantities of the hydrochloride salt can be processed in the manner indicated in Scheme 1 and observed in Figure 5.

The difference between Figure 2 and Figure 5 is attributed to the partitioning of HCl into the vapor phase and subsequent removal from the system in an open configuration. Anhydrous HCl is sparingly soluble in chlorobenzene,[1,8,28] but in a closed system, there will be a fixed concentration of HCl$_{(solv)}$ that will constrain equilibrium K_2 (Scheme 1). Thus, as evidenced in Figure 2, a closed system permits only a minor dissolution of the hydrochloride salt. In the open system employed here, HCl that partitions into the vapor phase is extracted from the system. Under these conditions, the dissolution rate is independent of time and exhibits zero-order kinetics.

The data points at 23 h in Figure 5 are less intense than that implied by the trend line for the CH_2 resonance at $t \geq 10$ h. As considered in the Experimental Section (section 2.2), single-point fluctuation in intensity was periodically observed upon application of the solvent suppression pulse sequence. A replicate run (not shown) exhibited constant CH_2 and NH_2

dx.doi.org/10.1021/ie403745s | Ind. Eng. Chem. Res. 2014, 53, 4156−4164

resonance intensities for $t \geq 10$ h, confirming complete dissolution of 4-BA.HCl$_{(s)}$ in the 10−24 h period.

4. KINETIC ANALYSIS

4.1. Development of a Kinetic Model. Kinetic models that correspond to the synthesis of polyurethanes have been developed. For example, Burkus and Eckert examined the kinetics of the triethylamine-catalyzed reaction of diisocyanates with 1-butanol in toluene.[29] Brock[30] and Di Giacomo[31] have analyzed the kinetics of the reaction of tolylene-2,4-diisocyanate with alcohols. More recently, Yang and co-workers have used ^{1}H NMR spectroscopy to determine kinetic parameters associated with the reaction of tolylene-2,4-diisocyanate and methanol.[32] However, no kinetic models are reported for the liberation of 4-BA from 4-BA.HCl$_{(s)}$ in chlorobenzene.

Although the kinetics for consecutive reactions displaying first-order kinetics are well-described,[26] the situation for consecutive mixed-order reactions is not documented as thoroughly. An exception is the work of Ball, who has derived expressions for a first-order first-stage process followed by a zero-order process.[33] However, to the best knowledge of the authors, no complete derivation is readily available for a consecutive process that proceeds via zero-order kinetics but is then followed by a first-order process. Consequently, a model is presented herein.

Let the concentrations of 4-BA.HCl$_{(s)}$, 4-BA.HCl$_{(solv)}$, and 4-BA$_{(solv)}$ at time t be respectively signified by the letters A, B, and C. Furthermore, a condition is set such that the concentration of A (A) is 0 and that of B is B_{max} at time t'. After time t', the concentration of B follows a first-order decay profile.

The consecutive reaction scheme is given by eq 16:

$$\mathrm{A} \xrightarrow[\text{zero-order}]{k_1} \mathrm{B} \xrightarrow[\text{first-order}]{k_2} \mathrm{C} \tag{16}$$

From the zero-order part of eq 16, the following expression holds: $dA/dt = -k_1$. Integrating and applying the initial condition ($A = A_0$ at $t = 0$), we get

$$A = -k_1 t + A_0 \tag{17}$$

until $A = 0$. If t' is the value of t when $A = 0$, $t' = A_0/k_1$.

The rate of formation of B until $t = t'$ is a competition between its formation from A and its decay to form C. When $t \leq t'$, $dB/dt = k_1 - k_2 B$. This first-order differential equation is solved using integrating factor $\exp(k_2 t)$.[34] The general solution is $B \exp(k_2 t) - (k_1/k_2) \exp(k_2 t) = c_1$, where c_1 is a constant. Applying the initial condition ($B = 0$ at $t = 0$), we have the following solution:

$$B = \frac{k_1}{k_2}[1 - \exp(-k_2 t)] \qquad \text{when } t \leq t' \tag{18}$$

When $t \geq t'$, the rate of decay of B is dependent only on the transition B → C. Thus, $dB/dt = -k_2 B$. This ordinary differential equation has the solution $B = c_2 \exp(-k_2 t)$, where c_2 is a constant.

Now, from the previous case (eq 18), we know that, at $t \leq t'$, $B = k_1[1 - \exp(k_2 t)]/k_2$. Hence $c_2 = (k_1/k_2)[\exp(k_2 t') - 1]$ and

$$B = \frac{k_1}{k_2}\{[\exp(k_2 t') - 1] \exp(-k_2 t)\} \qquad \text{when } t \geq t' \tag{19}$$

Consider product C from eq 16: $dC/dt = -k_2 B$ and it follows from eqs 18 and 19 that $dC/dt = k_1[1 - \exp(-k_2 t)]$ when $t \leq t'$, and $dC/dt = k_1[\exp(k_2 t') - 1] \exp(-k_2 t)$ if $t \geq t'$.

When $t \leq t'$, $dC/dt = k_1[1 - \exp(-k_2 t)]$. Integrating and applying the initial condition ($C = 0$ at $t = 0$) gives

$$C = \frac{k_1}{k_2}[t k_2 + \exp(-k_2 t) - 1] \qquad \text{when } t \leq t' \tag{20}$$

When $t \geq t'$, $dC/dt = k_1[\exp(k_2 t') - 1] \exp(-k_2 t)$, so $C = (-k_1/k_2)\{\exp(-k_2 t)\ [\exp(k_2 t') - 1]\} + c_3$ (where c_3 is a constant). From eq 20, $C = (k_1/k_2)[t' k_2 + \exp(k_2 t') - 1]$ at $t = t'$, and it follows that $c_3 = t' k_1$. Hence,

$$C = \frac{k_1}{k_2}\{[\exp(-k_2 t)][1 - \exp(k_2 t')] + t' k_2\}$$
$$\text{when } t \geq t' \tag{21}$$

4.2. Application of Kinetic Model. Using the solutions for the differential equations for this consecutive reaction sequence (eqs 17−21), a nonlinear least-squares analysis was employed to determine k_1 and k_2 and fitted to the experimental concentrations obtained from the NMR resonances (Figure 6). The turning point, t', is the time when the concentration of A is zero and the concentration of B is at a maximum. Thus, from Figure 5, $t' = 6.08$ h.

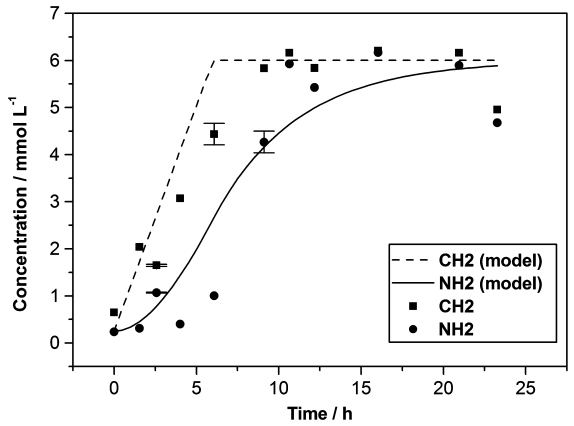

Figure 6. Concentrations associated with the CH_2 and NH_2 ^{1}H NMR signals for a mixture of 4-BA.HCl$_{(s)}$ and chlorobenzene at 373 K as a function of time in a stirred and open reactor. The concentrations associated with the CH_2 and NH_2 resonances are indicated by squares and circles, respectively. The error bars represent one standard deviation about the mean from four replicate measurements of standard solutions of 4-BA. The solid black line represents a fit of the calculated 4-BA$_{(solv)}$ concentration according to eqs 20 and 21. The dashed line represents the summation of 4-BA.HCl$_{(solv)}$ and 4-BA$_{(solv)}$, with the former quantity calculated via eqs 18 and 19.

The NH_2 concentrations represent experimentally obtained concentrations of 4-BA$_{(solv)}$. The black line is the nonlinear least-squares fit of eqs 20 and 21 to these data points, providing values for parameters k_1 and k_2 (see Table 1). The values for the two rate coefficients can then be substituted into eqs 18 and 19 in order to calculate the concentration profile for 4-BA.HCl$_{(solv)}$ over the full reaction coordinate. Adding this predicted concentration profile for 4-BA.HCl$_{(solv)}$ to the calculated value of NH_2 concentrations (Figure 6), the CH_2 concentrations can be predicted via eq 10. This quantity is plotted in Figure 6 as a dashed line and displays reasonable

dx.doi.org/10.1021/ie403745s | Ind. Eng. Chem. Res. 2014, 53, 4156−4164

Table 1. Rate Coefficients Defined According to Scheme 1 and Obtained from a Nonlinear Least Square Fit of Eqs 20 and 21 to the Concentration of 4-BA$_{(solv)}$ Determined for a Mixture of 4-BA.HCl$_{(s)}$ and Chlorobenzene at 373 K as a Function of Time in a Stirred and Open Reactor (Figure 6)[a]

rate coefficient	value
k_1	1.60 ($\pm$0.3) $\times$ 10^{-2} mmol dm^{-3} min^{-1}
k_2	3.30 ($\pm$0.7) $\times$ 10^{-3} min^{-1}

[a]The errors presented signify the range in k-values from duplicate experiments.

correspondence to the experimental dataset. Overall, Figure 6 shows the agreement between the predicted values for [4-BA.HCl$_{(solv)}$ + 4-BA$_{(solv)}$]$_t$, as signified by the CH_2 resonance, and [4-BA$_{(solv)}$]$_t$, as signified by the NH_2 resonance, to be reasonable.

The kinetic parameters presented in Table 1 are specific to the experimental arrangement employed. In order to optimize solubility values while avoiding thermal decomposition limits, as defined by the thermogravimetric measurements outlined in section 2, the consistency of the calculated kinetic and equilibrium constants, as a function of temperature, have not been examined. Furthermore, determination of the sensitivity of the kinetic parameters, as a function of mixing conditions, was deemed to be beyond the scope of the present investigation. Nevertheless, for the adopted experimental arrangements, the proposed model for the open system plus the derived rate coefficients provide a comprehensive description for a 4-BA liberation process as defined by Scheme 1.

The rate coefficients presented in Table 1 were combined with eqs 17−21 to determine the following parameters for the open reaction system over the full reaction coordinate: (i) the consumption of 4-BA.HCl$_{(s)}$ (eq 17), (ii) the formation/consumption of the intermediate 4-BA.HCl$_{(solv)}$ (eqs 18 and 19), and (iii) the formation of 4-BA$_{(solv)}$ (eqs 20 and 21). The resulting concentration profiles are presented in Figure 7. The point values for 4-BA.HCl$_{(solv)}$ calculated from eq 13 are also included in the figure and display a fair correspondence to the 4-BA.HCl$_{(solv)}$ profile. Figure 7 represents a comprehensive description of how a well-mixed open system can be employed to liberate 4-BA$_{(solv)}$ from 4-BA.HCl$_{(s)}$.

5. REACTION SCHEMES TO ACCOUNT FOR THE VARIABILITY OBSERVED BETWEEN CLOSED REACTION AND OPEN REACTION CONFIGURATIONS

Primarily because of their role in pharmaceutical science, there is a general interest in the solubility of hydrochloride salts and their dissociation in various solvents.[35,36] Furthermore, the solubility of aniline hydrochloride in protic solvents has been studied because of links to the manufacture of anhydrous magnesium chloride, which has application as a precursor for the production of magnesium metal produced by electrochemical methods.[37] However, despite the substantial resource requirement associated with the workup of the amine hydrochloride precipitate in certain large-scale isocyanate production units (eq 4),[1,3,5] little information is available in the open literature on the solubilization of relevant amine hydrochloride salts in representative process solvents such as chlorobenzene.[6,8] The present work examines this issue and shows the solubilization profile of a hydrochloride salt of a

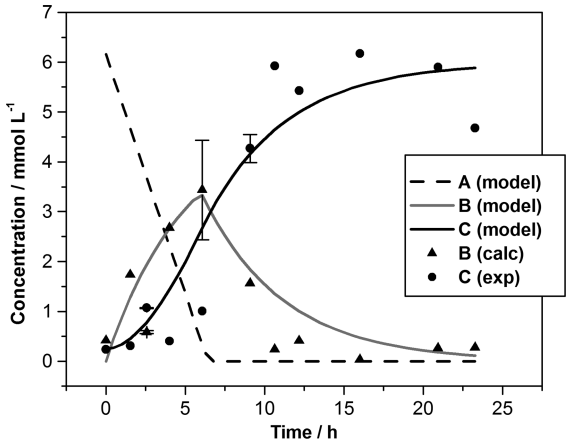

Figure 7. Concentrations associated with the NH_2 ^{1}H NMR signals (circles) for a mixture of 4-BA.HCl(*s*) and chlorobenzene at 373 K, as a function of time in a stirred and open reactor. The rate coefficients from Table 1 have been combined with eqs 17−21 to determine (a) the consumption of 4-BA.HCl$_{(s)}$ (dashed black line), (b) the concentration of 4-BA.HCl$_{(solv)}$ (solid gray line), and (c) the formation of 4-BA$_{(solv)}$ (solid black line). The point concentrations of 4-BA.Cl$_{(solv)}$ were calculated by application of eq 13 and are indicated by triangles. The error bars for [4-BA$_{(solv)}$] represent one standard deviation about the mean from four replicate measurements of standard solutions. The error bar shown for [4-BA.HCl$_{(solv)}$] corresponds to the range of maximum B concentration (B_{max}) values determined for a duplicate set of measurements.

model aromatic amine to be sensitive to the form of the reaction environment. For identical conditions of temperature and agitation rate, Scheme 2 illustrates the dramatic contrast between the profile observed when a closed reactor configuration is used (Scheme 2a and Figure 2) compared with an open reactor configuration (Scheme 2b and Figure 7).

Scheme 2. Reaction Schemes Applicable to (a) Closed Reaction Systems and (b) Open Reaction Systems

(a.) Closed reaction system

$$\text{4-BA.HCl}_{(s)} \overset{K_1}{\rightleftharpoons} \text{4-BA.HCl}_{(solv)}$$

(b.) Open reaction system

$$\text{4-BA.HCl}_{(s)} \overset{K_1}{\rightleftharpoons} \text{4-BA.HCl}_{(solv)} \overset{K_2}{\rightleftharpoons} \text{4-BA}_{(solv)} + \text{HCl}_{(solv)} \overset{K_3}{\rightleftharpoons} \text{4-BA}_{(solv)} + \text{HCl}_{(g)}$$

As noted above, it is assumed that the driving force for Scheme 2b is the entropically favored formation of gaseous hydrogen chloride. Tentatively, it is presumed that this process results in a free-energy change sufficient to overcome the favorable enthalpic term associated with the tight ion pair of the solvated hydrochloride salt. In the absence of this free-energy change, the limited solubility of 4-BA.HCl in chlorobenzene prevents the liberation of 4-BA, as witnessed in a closed reactor configuration.

6. CONCLUSIONS

A reaction scheme has been proposed from this laboratory study for the liberation of 4-BA from 4-BA.HCl$_{(s)}$ in chlorobenzene at 373 K. Solution phase ^{1}H NMR spectroscopy is used to analyze the composition of the liquid phase as a

dx.doi.org/10.1021/ie403745s | Ind. Eng. Chem. Res. 2014, 53, 4156−4164

function of time. The main results may be summarized as follows.

- In a "closed reaction" configuration, where HCl that has evolved from the dissociation of dissolved 4-BA.HCl is retained within the reactor headspace, the dissolution kinetics are shown to be first order. 4-BA.HCl$_{(solv)}$ saturates at 1.87 ($\pm$0.53) mmol dm^{-3}, with a rate coefficient of k_1 = 2.4 ($\pm$0.3) $\times$ 10^{-3} min^{-1}. No 4-BA$_{(solv)}$ forms under these conditions.
- In a "open reaction" configuration, where HCl that has evolved, originating from the dissociation of dissolved 4-BA.HCl, is vented from the reactor headspace, there is complete dissolution of 4-BA.HCl$_{(s)}$ to form 4-BA$_{(solv)}$. The dissolution process exhibits zero-order kinetics. Analysis of the ^{1}H NMR signals indicates 4-BA.HCl$_{(solv)}$ to be an intermediate species within a two-stage consecutive process, with the second stage exhibiting first-order kinetics. The overall process is entropically driven, via the partitioning of HCl into the gaseous phase from a solvated state.
- A kinetic model is derived for a two-stage consecutive process with the first stage exhibiting zero-order kinetics and the second stage exhibiting first-order kinetics. The model is applied to concentration measurements recorded from the open system and provides a good overall fit to the data. Rate coefficients for the first and second stages are determined to be 1.60 ($\pm$0.3) $\times$ 10^{-2} mmol dm^{-3} min^{-1} and 3.30 ($\pm$0.7) $\times$ 10^{-3} min^{-1}, respectively.
- The model for the open system is used to determine the following three parameters throughout the full reaction coordinate: (i) the consumption of 4-BA.HCl$_{(s)}$, (ii) the formation of the intermediate 4-BA.HCl$_{(solv)}$, and (iii) the formation of 4-BA$_{(solv)}$.

■ ASSOCIATED CONTENT

Supporting Information

Section S-1, Reaction vessel; Section S-2, Sensitivity of ^{1}H NMR measurements accessible via application of a solvent suppression pulse sequence; Section S-3, ^{1}H NMR calibration; Section S-4, A role for proton exchange in perturbing the peak shape of the ^{1}H NMR aromatic mine resonance in solutions of chlorobenzene; Section S-5, Impurity features observed in the ^{1}H NMR spectra. This material is available free of charge via the Internet at http://pubs.acs.org.

■ AUTHOR INFORMATION

Corresponding Author

*Tel.: (+44) (0)-141-330-4372. E-mail: David.Lennon@glasgow.ac.uk.

Notes

The authors declare no competing financial interest.

■ ACKNOWLEDGMENTS

Huntsman Polyurethanes are thanked for the provision of postgraduate studentship (E.K.G.). David Rycroft and Jim Gall (University of Glasgow) are thanked for their assistance with the NMR measurements. Stewart Parker (STFC ISIS Facility) provided assistance with ancillary vibrational calculations of 4-BA.HCl$_{(s)}$ and 4-BA$_{(s)}$, which helped to identify barriers to solvation.

■ REFERENCES

(1) Randall, D.; Lee, S. *The Polyurethanes Book*; John Wiley: Chichester, U.K., 2002.
(2) Weissermal, K.; Arpe, H.-J. *Industrial Organic Chemistry*, 3rd Edition; Wiley−VCH: Weinheim, Germany, 1997; p 377.
(3) Ulrich, H. Urethane Polymers. In *Kirk−Othmer Encyclopedia of Chemical Technology*, 4th Edition; Wiley: New York, 1997; pp 695−726.
(4) Richter, R. H.; Priester, R. D., Jr. Isocyanates, Organic. In *Kirk−Othmer Encyclopedia of Chemical Technology*, 4th Edition; Wiley: New York, 1997; pp 902−934.
(5) Ulrich, H. *Chemistry & Technology of Isocyanates*; John Wiley: Chichester, U.K., 1996.
(6) Gibson, E. K.; Winfield, J. M.; Muir, K. W.; Carr, R. H.; Eaglesham, A.; Gavezzotti, A.; Lennon, D. A structural and spectroscopic investigation of the hydrochlorination of 4,4′-methylenedianiline. *Phys. Chem. Chem. Phys.* **2010**, *12*, 3824−3833.
(7) Ding, J.; Hua, W.; Zhang, H.; Lou, Y. The development and application of two chlorine recycling technologies in polyurethane industry. *J. Clean. Prod.* **2013**, *41*, 97−104.
(8) Gibson, E. K.; Winfield, J. M.; Muir, K. W.; Carr, R. H.; Eaglesham, A.; Gavezzotti, A.; Parker, S. F.; Lennon, D. A structural and spectroscopic investigation of the hydrochlorination of 4-benzylaniline: The interaction of anhydrous hydrogen chloride with chlorobenzene. *Phys. Chem. Chem. Phys.* **2009**, *11*, 288−297.
(9) Badawi, H. A comparative study of the structure and vibrational spectra of diphenylmethane, the carcinogen 4,4-methylenedianiline and 4,4-methylenebis(*N*,*N*-dimethylaniline). *Spectrochim. Acta, A* **2013**, *109*, 213−220.
(10) Sutherland, I. W.; Hamilton, N. G.; Dudman, C. C.; Jones, P.; Lennon, D.; Winfield, J. M. Chlorination reactions relevant to the manufacture of trichloroethene and tetrachloroethene; Part 2: Effects of chlorine supply. *Appl. Catal., A* **2014**, *471*, 149−156.
(11) Abekawa, H.; Ito, Y.; Hibi, T. (Sumitomo). U.S. Patent No. 5,908,607, 1999.
(12) Wolf, A.; Mleczko, L.; Schlülter, O. F.; Schubert, S. (Bayer MaterialScience). Eur. Patent No. 2026905, 2006.
(13) López, N.; Gómez-Segura, J.; Marín, R. P.; Pérez-Ramírez, J. Mechanism of HCl oxidation (Deacon process) over RuO$_2$. *J. Catal.* **2008**, *225*, 29−39.
(14) Hevia, M. A. G.; Amrute, A. P.; Schmidt, T.; Pérez-Ramírez, J. Transient mechanism study of the gas-phase HCl oxidation of Cl$_2$ on bulk and supported RuO$_2$ catalysts. *J. Catal.* **2010**, *276*, 141−151.
(15) Mondelli, C.; Amrute, A. P.; Krumeich, F.; Schmidt, T.; Pérez-Ramírez, J. Shaped RuO$_2$/SnO$_2$−Al$_2$O$_3$ catalyst for large-scale stable Cl$_2$ production by HCl oxidation. *ChemCatChem.* **2011**, *3*, 657−660.
(16) Amrute, A. P.; Mondelli, C.; Moser, M.; Novell-Leruth, G.; Lopez, N.; Rosenthal, D.; Farra, R.; Schuster, M. E.; Teschner, D.; Schmidt, T.; Pérez-Ramírez, J. Performance, structure and mechanism of CeO$_2$ in HCl oxidation to Cl$_2$. *J. Catal.* **2012**, *286*, 287−297.
(17) Over, H.; Schomäcker, R. What makes a good catalysts for the Deacon process? *ACS Catal.* **2013**, *3*, 1034−1046.
(18) Dunlap, K. L. Phosgene. In *Kirk−Othmer Encyclopedia of Chemical Technology*, 4th Edition; Wiley: New York, 1997; pp 645−656.
(19) Mitchell, C. J.; van der Borden, W.; van der Velde, K.; Smit, M.; Scheringa, R.; Ahrika, K.; Jones, D. H. Selection of carbon catalysts for the industrial manufacture of phosgene. *Catal. Sci. Technol.* **2012**, *2*, 2109−2115.
(20) Zhang, T.; Troll, C.; Rieger, B.; Kintrup, J.; Schlüter, O. F.-K.; Weber, R. Reaction kinetics of oxychlorination of carbon monoxide to phosgene based on copper(II) chloride. *Appl. Catal., A* **2009**, *357*, 51−57.
(21) Zhang, T.; Troll, C.; Rieger, B.; Kintrup, J.; Schlüter, O. F.-K.; Weber, R. Composition optimization of silica-supported copper(II) chloride substance for phosgene production. *Appl. Catal., A* **2009**, *365*, 20−27.
(22) Zhang, T.; Troll, C.; Rieger, B.; Kintrup, J.; Schlüter, O. F.-K.; Weber, R. Oxychlorination of CO to phosgene in a three-step reaction

cycle and corresponding catalytic mechanism. *J. Catal.* **2010**, *270*, 76−85.
(23) Cavani, F. Catalytic selective oxidation: The forefront in the challenge for a more sustainable chemical industry. *Catal. Today* **2010**, *157*, 8−15.
(24) Freeman, R. *A Handbook of Nuclear Magnetic Resonance*; Longman: Harlow, U.K., 1987.
(25) Guéron, M.; Plateau, P.; Decorps, M. Solvent signal suppression in NMR. *Prog. NMR Spect.* **1991**, *23*, 135−209.
(26) Frost, A. A.; Pearson, R. G. *Kinetics and Mechanism*; John Wiley: New York, 1961.
(27) Khairuzzaman, A.; Ahmed, S. U.; Savva, M.; Patel, N. K. Zero-order release of aspirin, theophylline and atenolol in water from novel methylcellulose glutarate matrix tablets. *Int. J. Pharm.* **2006**, *318*, 15−21.
(28) Fogg, P. G. T.; Gerrard, W. *Solubility of Gases in Liquids: A Critical Evaluation of Gas/Liquid Systems in Theory and Practice*; John Wiley: Chichester, U.K.; 1991.
(29) Burkus, J.; Eckert, C. F. The kinetics of the triethylamine-catalyzed reaction of diisocyanates with 1-butanol in toluene. *J. Am. Chem. Soc.* **1958**, *80*, 5948−5950.
(30) Brock, F. H. Kinetics of the 2,4-tolylene diisocyanate−alcohol reaction. *J. Phys. Chem.* **1961**, *65*, 1638−1639.
(31) Di Giacomo, A. The reaction of toluene-2,4-diisocyanate with *n*-butyl alcohol. *J. Phys. Chem.* **1961**, *65*, 696−697.
(32) Yang, P. F.; Han, Y. D.; Li, T. D.; Li, J. Y. ^{1}H NMR analysis of the tolylene-2,4-diisocyanate−methanol reaction. *Chin. Chem. Lett.* **2010**, *21*, 853−855.
(33) Ball, D. W. Kinetics of consecutive reactions: First reaction, first-order; second reaction, zeroth-order. *J. Chem. Educ.* **1998**, *75*, 917−919.
(34) Tebutt, P. *Basic Mathematics for Chemists*; John Wiley: New York, 1998.
(35) Serajuddin, A. T. M.; Jarowski, C. I. Effect of diffusion layer pH and solubility on the dissolution rate of pharmaceutical bases and their hydrochloride salts, I: Phenazopyridine. *J. Pharm. Sci.* **1985**, *74*, 142−147.
(36) Silkov, A. A. Conductometric determination of anilinium ion dissociation constants at various temperatures. *Russ. J. Phys. Chem.* **1999**, *73*, 1224−1228.
(37) Sun, S.; Li, Z. Experimental Measurement and Modeling of Aniline Hydrochloride Solubility in Water, Methanol, Ethanol, Propan-1-ol, and Their Mixed Systems. *J. Chem. Eng. Data* **2012**, *57*, 219−226.